iScience

CellPress

Article

Aversion or Salience Signaling by Ventral Tegmental Area Glutamate Neurons

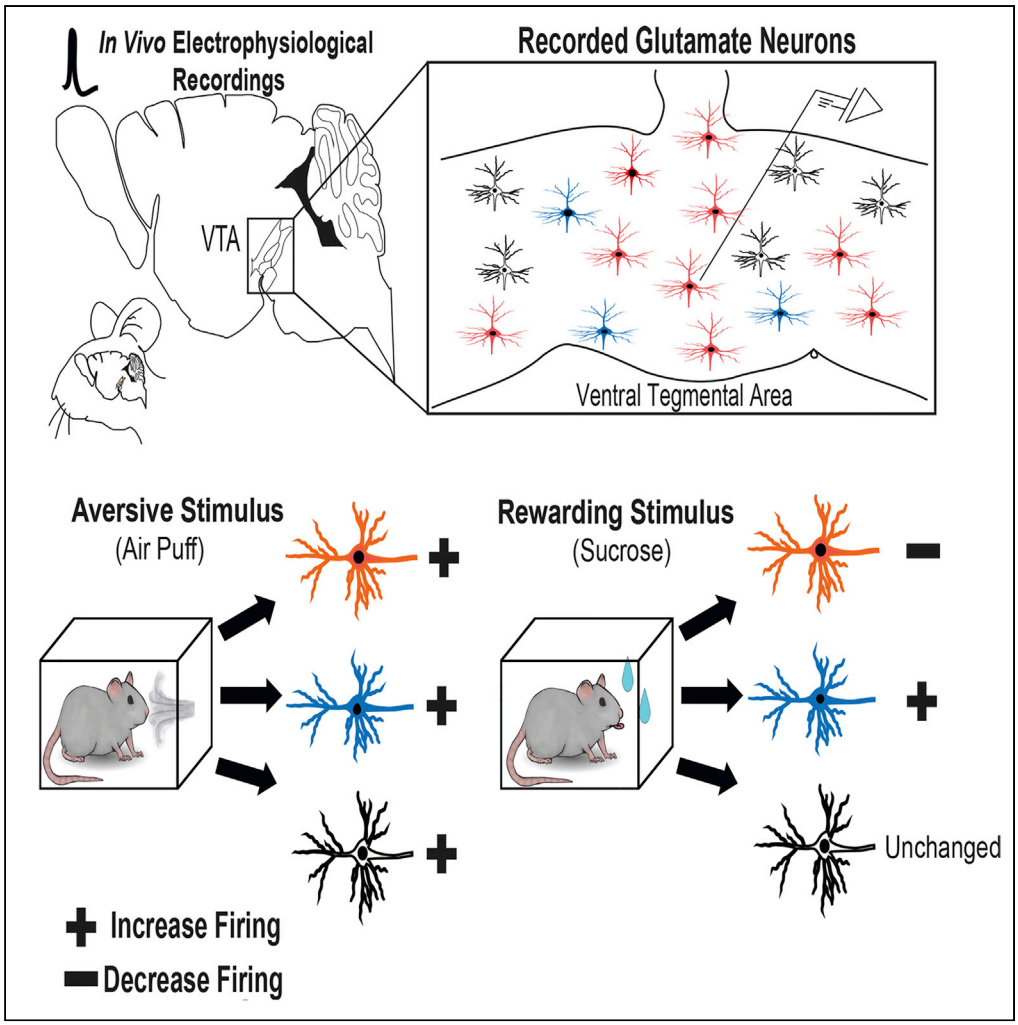

David H. Root,
David J. Estrin,
Marisela Morales

mmorales@intra.nida.nih.gov

HIGHLIGHTS

The majority of VTA glutamate neurons increase their firing during airpuff

The majority of VTA glutamate neurons decrease their firing during reward

A few VTA glutamate neurons increase their firing during both airpuff and reward

Firing heterogeneity among VTA glutamate neurons during reward delivery or omission

Root et al., iScience 2, 51–62
April 27, 2018
https://doi.org/10.1016/j.isci.2018.03.008

iScience

CellPress

Article

Aversion or Salience Signaling by Ventral Tegmental Area Glutamate Neurons

David H. Root,[1,2] David J. Estrin,[1] and Marisela Morales[1,3,*]

SUMMARY

Ventral tegmental area (VTA) neurons play roles in reward and aversion. The VTA has, in addition to dopamine neurons, glutamatergic neurons expressing VGluT2. Here, by determining the firing patterns of VTA-VGluT2 neurons expressing channelrhodopsin 2, we identified a major subpopulation of VTA-VGluT2 neurons whose firing rates decreased or were unchanged during sucrose consumption and increased during facial airpuff presentation. We identified a small subpopulation of VTA-VGluT2 neurons whose firing rates increased in response to both rewarding and aversive stimuli. We also found that the changes in firing rate of some VTA-VGluT2 neurons were greater following reward delivery compared with reward omission, whereas others did not differ. We conclude that VTA-VGluT2 neurons are responsive to aversive stimuli, but subpopulations of VTA-VGluT2 neurons are differentially affected by sucrose reward. Reward-responsive subpopulations of VTA-VGluT2 neurons are also divided into those affected by reward expectation alone or the real-time delivery of reward.

INTRODUCTION

The ventral tegmental area (VTA) plays crucial roles in the processing of both rewarding and aversive stimuli (Bromberg-Martin et al., 2010; Lammel et al., 2014; Wise, 2004; Barker et al., 2016). The VTA contains several different types of neurotransmitter-releasing neurons that each play causal roles in reward or aversion (Root et al., 2014a; van Zessen et al., 2012; Lammel et al., 2012; Tan et al., 2012). Among the most recently described neurons of the VTA are those expressing vesicular glutamate transporter 2 (VGluT2), which release the excitatory neurotransmitter glutamate (Yamaguchi et al., 2007). VTA VGluT2 neurons are a collection of molecularly heterogeneous neurons mostly found within the midline aspects of the VTA in mouse, rat, nonhuman primate, and human (Yamaguchi et al., 2007, 2011, 2015; Root et al., 2014b, 2016; Viereckel et al., 2016; Zhang et al., 2015). Subsets of VTA VGluT2 neurons solely release glutamate, whereas others co-release glutamate and dopamine (Zhang et al., 2015) or glutamate and GABA (Root et al., 2014b). Although multiple types of VTA VGluT2 neurons may target the same output structure, it has so far been shown that VGluT2-only neurons project to nucleus accumbens shell, and VGluT2-GABA neurons project to the lateral habenula (Qi et al., 2016; Root et al., 2014b). VTA VGluT2 neurons have, in addition to their molecular heterogeneity, diverse roles in reward or aversion. Behavioral studies have shown that optogenetic activation of VTA VGluT2 neurons or their axonal terminals elicit aversive or rewarding responses (Root et al., 2014a; Lammel et al., 2015; Wang et al., 2015; Yoo et al., 2016; Qi et al., 2016). However, the patterns of neuronal activity or synchronization induced by optogenetic activation may not occur under physiological conditions. Thus, to determine the participation of individual VTA VGluT2 neurons in reward or aversion under physiological conditions, we determined the changes in firing rate of optogenetically phototagged VTA VGluT2 neurons in response to sucrose reward or an aversive airpuff stimulus in freely moving mice.

We found that, although most VTA VGluT2 neurons decreased their firing rates during sucrose consumption, a few VTA VGluT2 neurons increased their firing rates. We also found that, although the firing rates of some VTA VGluT2 neurons changed only by the presence of the delivered reward, the firing rates of others did not differ by the presence or omission of the reward. Regarding responses by VTA VGluT2 neurons to the aversive stimulus, we found that the firing rates of most VTA VGluT2 neurons increased in response to airpuff, including those neurons whose firing rates were increased in response to sucrose reward. Based on our results from single-cell *in vivo* recordings, we conclude that VTA VGluT2 neurons are heterogeneous in their function. We suggest that, under physiological conditions, most VTA VGluT2 neurons signal aversion, whereas some VTA VGluT2 neurons signal salient stimuli.

[1]Neuronal Networks Section, Integrative Neuroscience Research Branch, National Institute on Drug Abuse, 251 Bayview Boulevard Suite 200, Baltimore, MD 21224, USA

[2]Present address: Department of Psychology and Neuroscience, University of Colorado Boulder, 2860 Wilderness Place, Boulder, CO 80301 USA

[3]Lead Contact

*Correspondence: mmorales@intra.nida.nih.gov

https://doi.org/10.1016/j.isci.2018.03.008

RESULTS

In Vivo Recordings of VTA VGluT2 Neurons

We injected a Cre-dependent adeno-associated viral vector encoding channelrhodopsin2 (ChR2) tethered to eYFP into the VTA of VGluT2-IRES::Cre mice (VGluT2-ChR2 mice; Figure 1A). Three weeks later, we implanted into the VTA of these VGluT2-ChR2 mice an organized array of stainless steel microwires, which were surrounded by an optical fiber (Figure 1B). We trained mice on a reward task in which sucrose delivery was paired with a CS^+, but not paired with a CS^- (Figure 1C). We compared the percentage of reward port entries in response to each cue on their first day of training with that on the recording day, which occurred at a minimum of the third day of training. This comparison yielded a significant cue × day interaction, $F(1,13) = 56.24$, $p < 0.001$. Pairwise comparisons indicated that, VGluT2-ChR2 mice did not differ in reward port entries in response to either cue on day 1 ($p > 0.05$), whereas VGluT2-ChR2 mice showed significantly greater reward port entries in response to the CS^+ compared with the CS^- on the recording day ($p < 0.001$) (Figure 1D). The discrimination between CS^+ and CS^- cues by VGluT2-ChR2 mice on the recording day was learned, as indicated by significantly more reward port entries for the CS^+ on the recording day (at least 3 days of training) than on the first day of training ($p < 0.05$) and significantly fewer reward port entries for the CS^- ($p < 0.01$) (Figure 1D).

Of 246 recorded midbrain neurons, 27 neurons were confirmed to be within the VTA and were optogenetically classified as VGluT2 neurons based on their short latency (mean and SEM: 7.80 ± 0.56 ms) and high fidelity (mean and SEM: 0.86 ± 0.03) firing in response to 5-ms pulses of 473 nm light (n = 27, Figures 1E and 1F). We did not detect among the recorded VTA VGluT2 neurons differences between light-evoked waveforms or spontaneous waveforms (Figure 1G). We established the distribution of VGluT2 recorded neurons within the VTA by postmortem detection of the tips of the micro-electrode array among the tyrosine-hydroxylase-positive neurons (Figure 1H). Recorded VTA VGluT2 neurons were localized to the rostral linear nucleus (n = 13 neurons from 9 microwires), parabrachial pigmented nucleus (n = 10 neurons from 8 microwires), and the paranigral nucleus (n = 4 neurons from 4 microwires) (Figure 1I). We found that VTA VGluT2 neurons had diverse waveform characteristics and a wide range of baseline firing rates between 0.5 and 34.4 Hz (mean ± SEM: 9.1 ± 1.6 Hz).

Firing Rates of VTA VGluT2 Neurons Following Reward Delivery

To determine possible responses of VTA VGluT2 neurons to sucrose reward, we first compared the changes in firing rate of VTA VGluT2 neurons following reward port entries during CS^+ trials (paired with sucrose delivery) with changes in firing rate following reward port entries during CS^- trials (not paired with sucrose delivery) (Figure 2A). We found that following reward port entry on CS^+ trials, about half of the recorded VTA VGluT2 neurons (n = 13/27) showed at least a 50% decrease in firing rate, whereas about 10% of VTA VGluT2 neurons (n = 3/27) showed at least a 50% increase in firing rate (Figures 2B and 2C). The changes in firing rate of VTA VGluT2 neurons following CS^+ reward port entry were significantly greater than the changes in firing rate following reward port entry during CS^- trials, $t(26) = -4.41$, $p < 0.001$ (Figures 2D and 2E).

The diminished changes in firing rate of VTA VGluT2 neurons following reward port entry during CS^- trials compared with CS^+ trials may reflect different reward expectations or responses to the absence of the reward during CS^- trials. To differentiate between these two possibilities, we compared the changes in firing rate of VTA VGluT2 neurons following reward port entry during the 90% of CS^+ trials that resulted in sucrose delivery against the 10% of error trials (CS^E) in which the CS^+ was played but did not result in sucrose delivery (Figure 2A). We found that as a group, VTA VGluT2 neurons had a significantly greater change in firing rate following reward port entry during CS^+ trials compared with CS^E trials, $t(24) = -2.94$, $p < 0.01$ (Figures 2F–2J). However, by a direct comparison of individual neurons' firing rates following reward port entries for CS^+ or CS^E trials, we found that 55.56% of VTA VGluT2 neurons (n = 15) had less than a 50% difference in firing rate between these events (Figures 2F and 2G), suggesting that a subpopulation of VTA VGluT2 neurons is responsive to reward expectation regardless of its delivery. In contrast, 44.44% of VTA VGluT2 neurons (n = 12) had at least a 50% difference in firing rate following reward port entry for CS^+ or CS^E trials (Figures 2I and 2J), suggesting that a different subpopulation of VTA VGluT2 neurons is responsive to the presence of reward but not to its absence.

Firing Rates of VTA VGluT2 Neurons before Reward

Through video analysis of the times at which mice approached the reward port, we determined whether the changes in firing rate of VTA VGluT2 neurons were related to motor behavior before the receipt of the

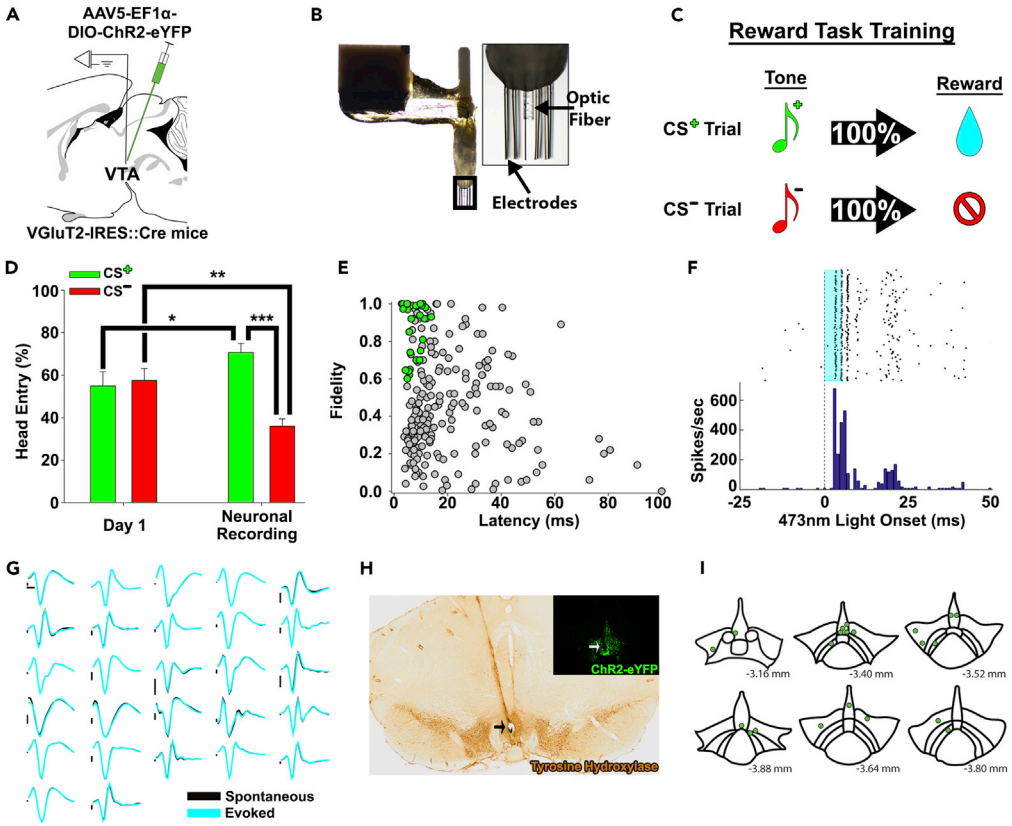

Figure 1. Recording of VTA VGluT2 Neurons during a Sucrose Reward Task

(A) VGluT2-IRES::Cre mice were injected in VTA with AAV5-EF1α-DIO-ChR2-eYFP.

(B) Sixteen-channel stainless steel microwire array that was implanted in the VTA for neuronal recordings. Inset shows optical fiber and electrodes.

(C) Mice were trained on a sucrose reward task. During training, sucrose delivery was paired to the CS^+ tone but not to the CS^- tone.

(D) Mice learned to make reward port entries in the sucrose delivery port in response to the CS^+ significantly more than to the CS^- on the recording day (minimum third day of training), when compared with the first day of training. When two recordings were performed, recording day behavioral data reflect the average performance over both recording days. Data are mean ± SEM.

(E) Scatterplot of all recorded neurons with median latency to fire an action potential following onset of photostimulation and fidelity to fire an action potential within 100 ms following onset of photostimulation (5 ms, 10–20 mW). Optogenetically identified VTA VGluT2 that met criteria (green dots) and those that did not meet criteria or were outside the VTA (gray dots).

(F) Optogenetically identified VTA VGluT2 neuron. Raster and histogram are centered on photostimulation (blue rectangle; 5 ms, 15 mW) onset (time 0), and each dot representing an action potential.

(G) Mean action potential waveforms of VTA VGluT2 neurons before photostimulation (spontaneous; black tracings) and following photostimulation onset (evoked, cyan tracings). Black vertical scale bars, 100 μV, horizontal scale bar, 200 μs.

(H) VTA localized microwire (blue spot surrounded by lesioned tissue) within the VTA, as delineated by tyrosine hydroxylase-immunoreactivity (brown). Inset shows the same section, before tyrosine hydroxylase immunoreactivity, under fluorescence microscopy showing ChR2-eYFP expression. Arrow identifies VTA localized microwire surrounded by ChR2-eYFP (inset) and tyrosine hydroxylase immunoreactivity.

(I) Localization of microwires that recorded each optogenetically identified VGluT2 neuron (green dots) within the VTA. *$p < 0.05$, **$p < 0.01$, ***$p < 0.001$.

reward, or in response to the CS^+ or CS^- cues. We found that 29.6% of VTA VGluT2 neurons (n = 8/27) had at least a 50% change in firing rate during approaches to the reward port while the CS^+ was played (Figures 3A and 3B). For those neurons that lack approach-related responses and change firing rate following reward port entry (while the CS^+ was played), the changes in firing rate began at the offset of the approach that coincided with reward receipt (Figures 3C and 3D). Thus the analysis of the approach-related firing appears useful for predicting the responsivity of VTA VGluT2 neurons to reward.

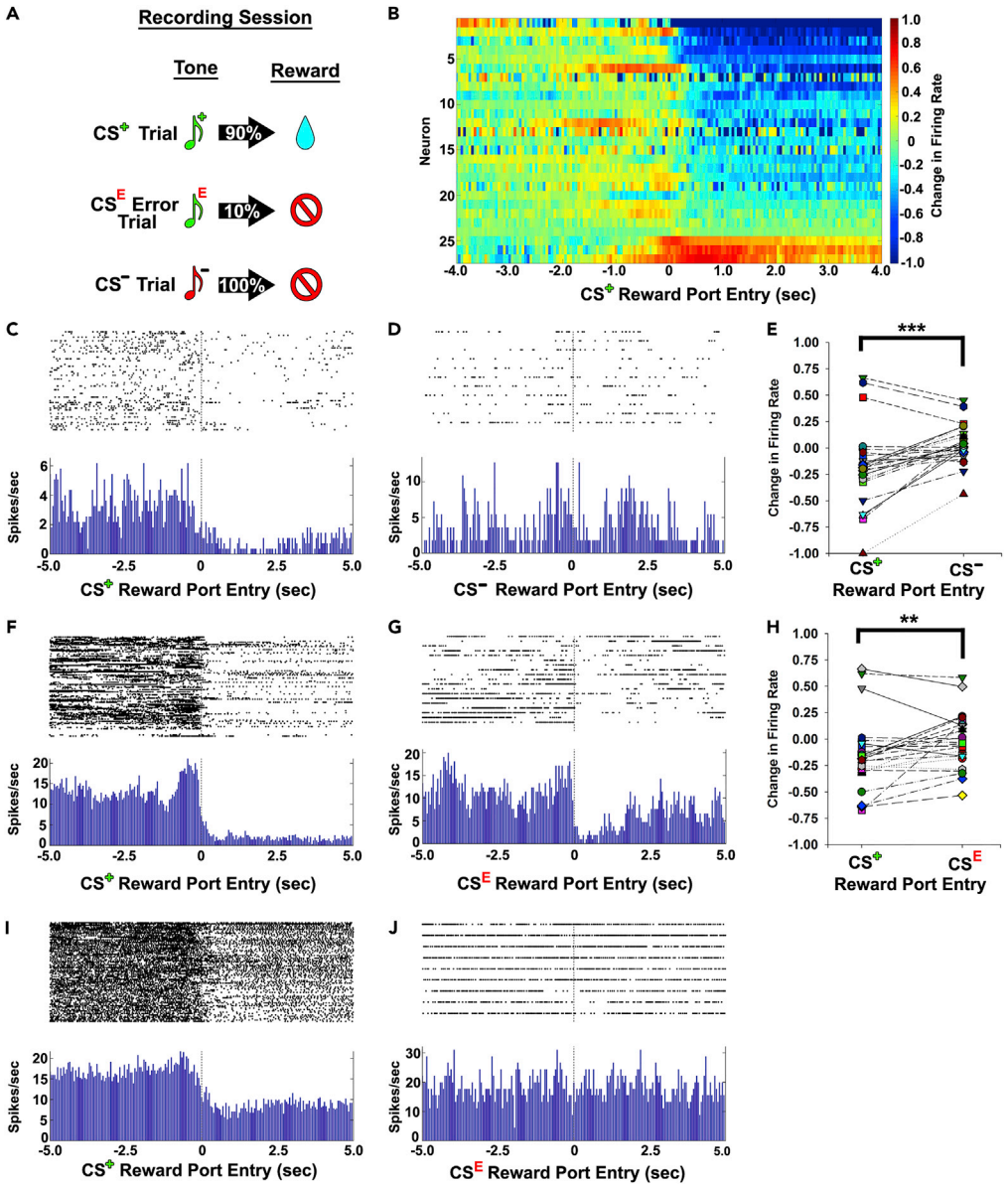

Figure 2. Subpopulations of VTA VGluT2 Neurons Decrease or Increase Firing Rate at Reward

(A) Reward task during recordings in which 90% of the CS^+ presentations resulted in sucrose delivery; the remaining 10% of CS^+ presentations did not result in sucrose delivery (referred as CS^E), and 100% of CS^- trials did not result in sucrose delivery.

(B) Changes in firing rate of each recorded VTA VGluT2 neuron before and after reward port entries during CS^+ trials (paired to sucrose delivery) (time 0).

(C and D) (C) VTA VGluT2 neuron showing a decrease in firing rate following reward port entry during CS^+ trials (time 0). (D) The same neuron showing a reduced decrease in firing rate following reward port entry during CS^- trials (entry = time 0).

(E) VTA VGluT2 neurons had a significantly greater change in firing rate following reward port entry during CS^+ trials compared with CS^- trials.

(F and G) (F) VTA VGluT2 neuron showing a decrease in firing rate following reward port entry during CS^+ trials (time 0). (G) The same neuron showing a similar decrease in firing rate following reward port entry during CS^E trials (entry = time 0).

(H) VTA VGluT2 neurons had a significantly greater change in firing rate following reward port entry during CS^+ trials compared with CS^E trials.

(I and J) (I) VTA VGluT2 neuron showing a decrease in firing rate following reward port entry during CS^+ trials (time 0). (J) The same neuron showing no change in firing rate following reward port entry during CS^E trials (entry, time 0).

***$p < 0.001$, **$p < 0.01$, ns not significant.

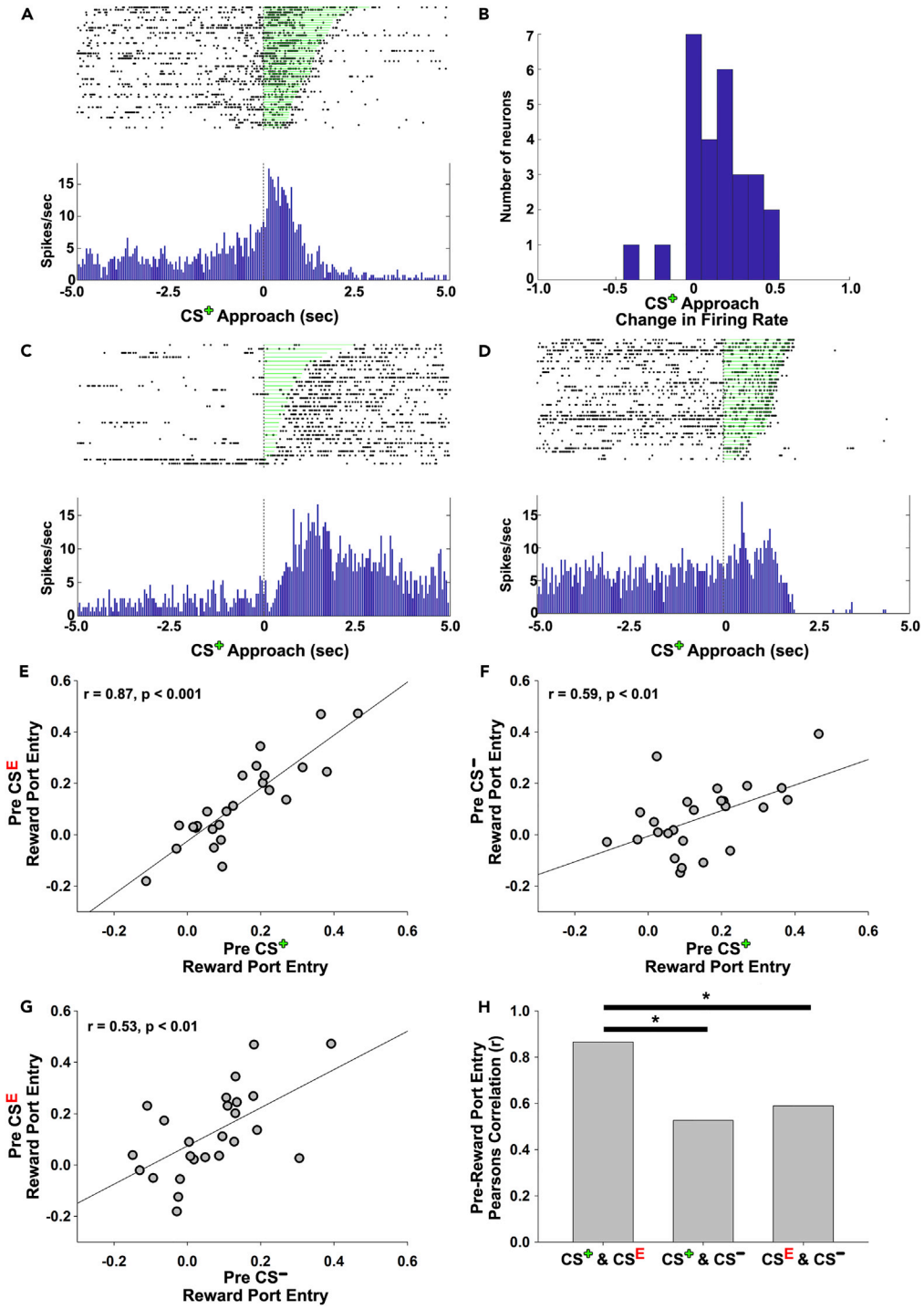

Figure 3. A Subpopulation of VTA VGluT2 Neurons Changes Firing Rate during Approaches to Retrieve Rewards

(A) VTA VGluT2 neuron showing an increase in firing rate during approaches to the reward port during CS^+ trials. Approach duration is shaded in green, with approach onset at time 0 and end of green shading the offset of approach in which the reward port was entered.

(B–D) (B) Distribution of VTA VGluT2 neuron changes in firing rate during the CS^+ approach. Most approach-related firing rates were increases from baseline. VTA VGluT2 neurons that decreased (C) or increased (D) their firing rates at the approach offset, which coincided with reward consumption.

Figure 3. *Continued*
(E–G) Correlation of changes in firing rate between pre-reward port entry during CS^+ and CS^E trials (E), pre-reward port entry during CS^+ and CS^- trials (F), and pre-reward port entry during CS^- and CS^E trials (G).
(H) Correlation coefficients of changes in firing rate for pre-reward port entry during CS^+ and CS^E trials, CS^- and CS^E trials, and CS^- and CS^E trials. A significantly stronger correlation was found between changes in firing rate before reward port entries for CS^+ and CS^E compared with correlations involving CS^-.
*$p < 0.05$.

We further assessed whether the changes in firing rate before reward port entry differed with reward expectation by comparing the correlations of changes in firing rate during the two seconds before reward port entry for CS^+, CS^E, or CS^- trials. Pre-reward port entry was used as a node for these analyses because some neurons had less than five video-scored approach movements for CS^- or CS^E trials. Changes in firing rate were significantly correlated for all pre-reward port entry conditions (Figures 3E–3G). However, the correlation of changes in firing rate before reward port entry for CS^+ or CS^E trials was significantly greater than the correlation between changes in firing rate before CS^+ or CS^- reward port entries ($z = -2.45$, $p < 0.05$), as well as for the correlation of changes in firing rate before CS^- or CS^E reward port entries ($z = 2.29$, $p < 0.05$) (Figures 3E and 3F). Thus the changes in firing rate by VTA VGluT2 neurons related to reward-seeking behavior differ when the CS^+ is played versus the CS^-, suggesting that the approach-related firing is sensitive to reward expectancy.

We next determined whether VTA VGluT2 neurons were responsive to learned cues and found that 11.11% of the recorded neurons (n = 3/27) showed at least a 50% change in firing rate from baseline in response to both the CS^+ and CS^- (Figure 4A). Only one neuron had CS^+ evoked firing that was clearly greater than the CS^- evoked response (Figures 4B and 4C). A different subpopulation of recorded VTA VGluT2 neurons (n = 5/27) had at least a 50% change in firing rate in response to only the CS^- (Figures 4D and 4E).

Firing Rates of VTA VGluT2 Neurons during Aversion

We determined whether the same VTA VGluT2 neurons previously recorded during the reward task (see earlier discussion) were responsive to an aversive stimulus by recording their firing rate in response to an airpuff stimulus (Figure 5A). We found that over three-quarters of the recorded neurons (n = 23/27) had at least a 50% increase in firing rate during the airpuff compared with baseline (Figures 5B and 5C). We detected a significant increase in baseline firing rates in response to consecutive airpuff stimuli compared with the cue baseline recorded during the reward task, $t(26) = -2.18$, $p < 0.05$ (Figure 5D). Thus it appears that VTA VGluT2 neurons not only increased their firing rate in response to airpuff, but also entered an elevated state of firing during the consecutive airpuffs. To determine how single VTA VGluT2 neurons respond to both rewarding and aversive stimuli, we compared their changes in firing rate following reward port entry during CS^+ trials and changes in firing rate during the airpuff stimulus. By a hierarchical cluster analysis, we detected two subpopulations of VTA VGluT2 neurons. We found that, although most VTA VGluT2 neurons had firing rates less than or equal to baseline during reward and increased firing rates during airpuff stimuli (n = 24/27), approximately 10% of the neurons increased their firing rates during both rewarding and aversive events (n = 3/27) (Figure 5E).

DISCUSSION

VTA VGluT2 neurons are diverse in their molecular composition (Kawano et al., 2006; Yamaguchi et al., 2007, 2011; Root et al., 2014b), efferent projections (Yamaguchi et al., 2007, 2011; Root et al., 2014b; Taylor et al., 2014), and synaptic connectivity (Dobi et al., 2010; Root et al., 2014b; Wang et al., 2015; Qi et al., 2016). In addition, optogenetic studies have implicated VTA VGluT2 neurons in a variety of motivational states, including aversion (Root et al., 2014a; Lammel et al., 2015; Lecca et al., 2017; Qi et al., 2016), reward (Wang et al., 2015; Yoo et al., 2016), perseveration (Kabanova et al., 2015), depression (Qi et al., 2016), and sociability (Krishnan et al., 2017). Here, consistent with the molecular, circuit, and functional diversity among VTA VGluT2 neurons, we demonstrate that there are subpopulations of VTA VGluT2 neurons whose firing rates are altered by sucrose reward, airpuff delivery, learned cues, or reward approach movements.

VTA neurons expressing VGluT2 are in close proximity to neighboring areas containing high concentrations of VGluT2 neurons (e.g., red nucleus, supramammillary nucleus, medial terminal nucleus of the accessory optic tract found in the VTA and surrounding areas) (Yamaguchi et al., 2007). Thus we utilized fixed organized arrays of stainless steel microelectrodes surrounded by an optic fiber to unambiguously record

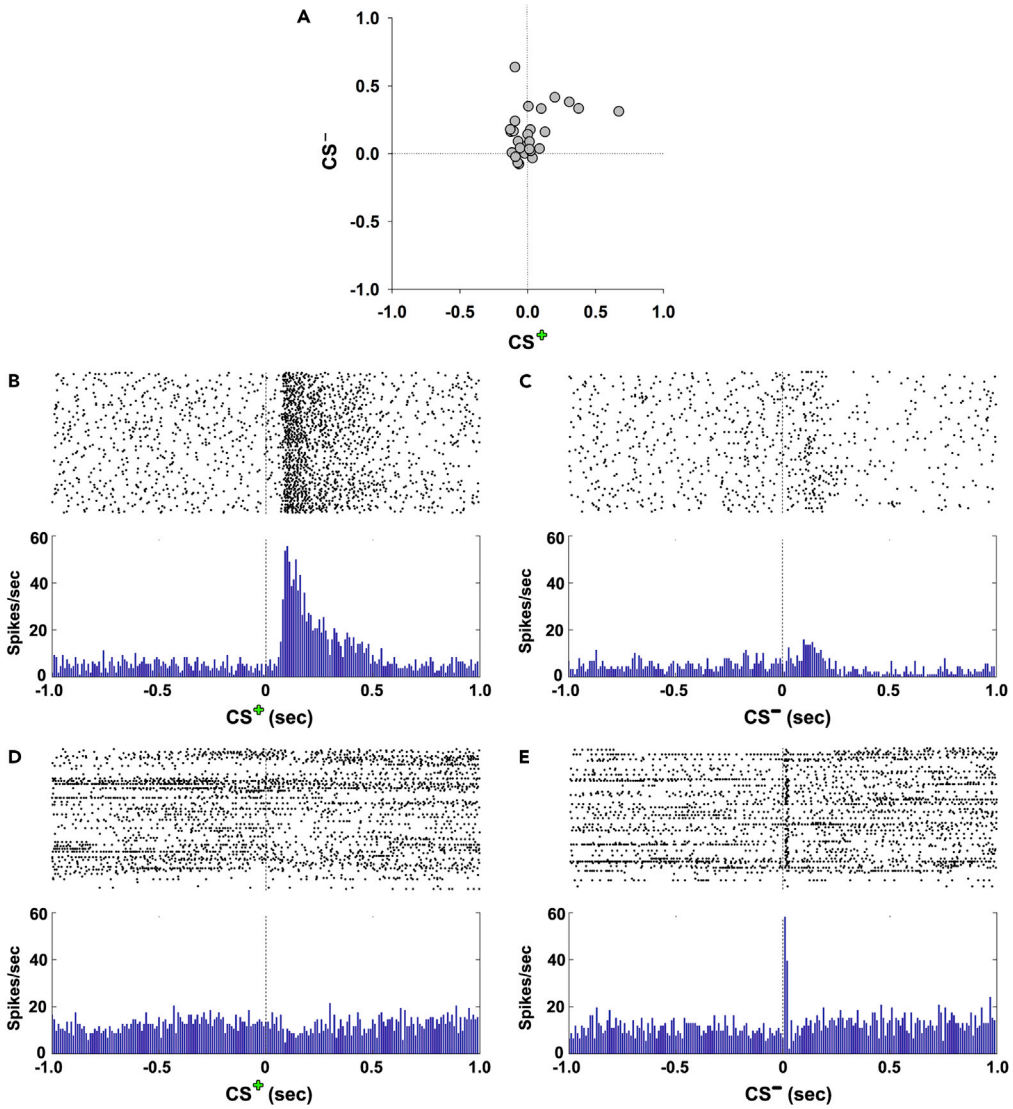

Figure 4. A Subpopulation of VTA VGluT2 Neurons Are Cue Responsive

(A) Scatterplot of VTA VGluT2 neuron changes in firing rate evoked by the CS^+ or CS^-.

(B and C) A single VTA VGluT2 neuron that increased its firing rate at least 50% from baseline in response to both the CS^+ (B) and CS^- (C). The CS^+ evoked response is clearly stronger than the CS^- evoked response.

(D and E) A single VTA VGluT2 neuron that was unresponsive to the CS^+ (D) but increased its firing rate at least 50% from baseline in response to the CS^- (E).

VGluT2 neurons located within the VTA. Although this approach allows the precise localization of individual microelectrodes within or outside the VTA, the light is delivered more strongly to microwires proximal to the fiber and less strongly to those distal to the fiber. In addition to light intensity, VTA VGluT2 neurons are known to be significantly more hyperpolarized than other VTA neurons (Hnasko et al., 2012). Thus these two factors may potentially contribute to the difficulty in the optogenetic identification of VTA glutamatergic neurons when compared with other VTA cell types. In our recordings, we considered a neuron to be ChR2 responsive when the neuron had at least 60% fidelity to fire an action potential in response to 5 ms of 473 nm light and a response latency below 15 ms, as previously implemented by Kravitz and colleagues using fixed organized arrays of microelectrodes (Kravitz et al., 2013). However, other methods and criteria have been used for identifying ChR2-mediated responsive neurons (Cohen et al., 2012; Nieh et al., 2015; Stauffer et al., 2016; Kravitz et al., 2013; Zhang et al., 2013). We found a mean latency of 7.8 ms for VTA VGluT2 ChR2-responsive neurons. This latency duration is similar to that reported of

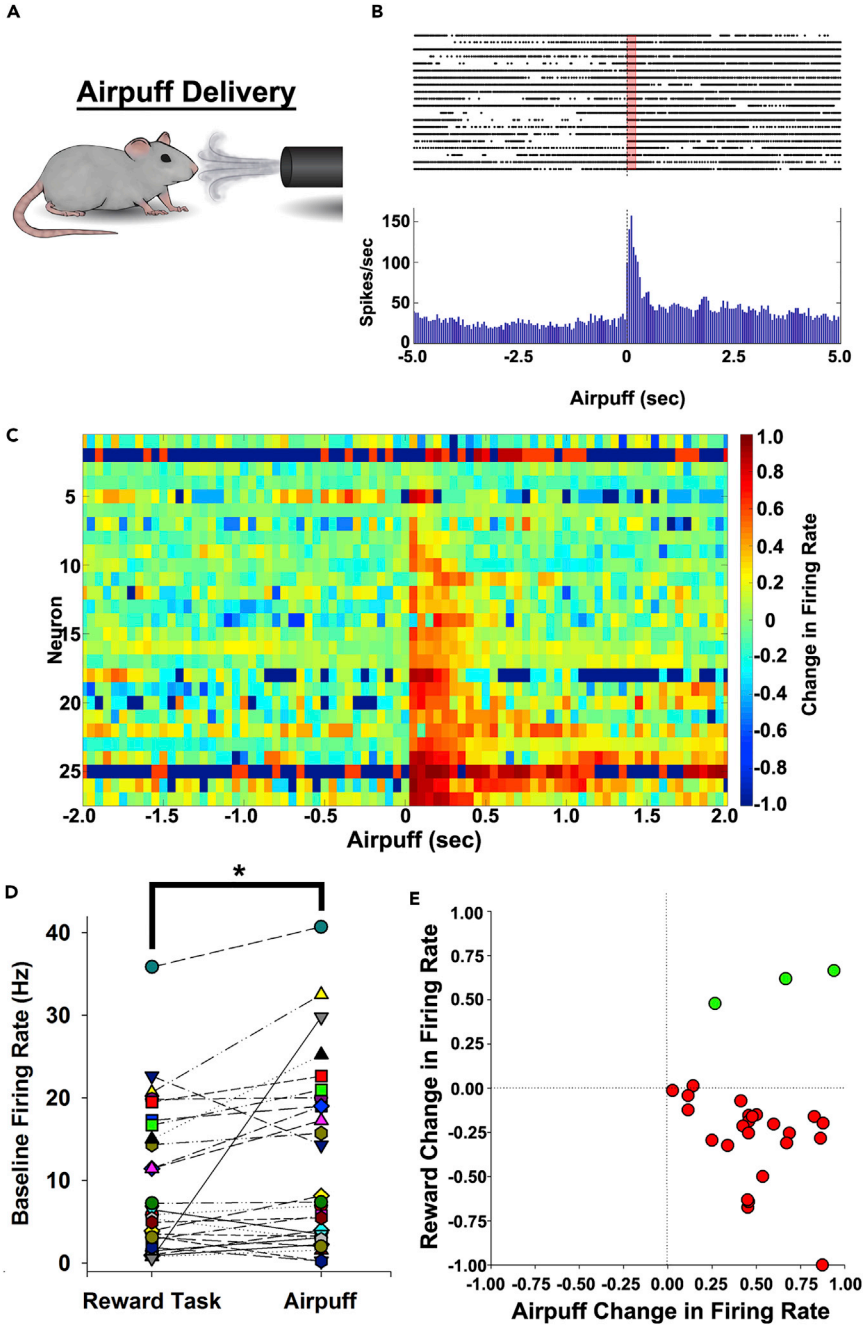

Figure 5. A Large Subpopulation of VTA VGluT2 Neurons Increases Firing Rate in Response to Airpuff Delivery

(A) Mice received consecutive airpuffs following the reward task.

(B) VTA VGluT2 neuron showing an increase in firing rate in response to airpuff stimulus (time 0). Airpuff duration is shaded in red.

(C) Changes in firing rate of each recorded VTA VGluT2 neuron in response to the airpuff (onset, time 0). Color indicates change in firing rate from baseline (0 is no change from baseline; negative values are decreases in firing rate from baseline, and increasing values are increases in firing rate from baseline).

(D) Baseline firing rates were significantly elevated during consecutive airpuffs compared with the cue baseline during the reward task.

Figure 5. *Continued*

(E) Scatterplot of VTA VGluT2 neuron changes in firing rate during airpuff delivery and following reward port entry during CS^+ trials paired to sucrose delivery. Two subpopulations of VTA VGluT2 neurons were identified by cluster analysis, those increasing their firing rate in response to both reward and airpuff (green dots) and those increasing their firing rates in response to the airpuff but decreasing or not changing their firing rates in response to reward (red dots).

*$p < 0.05$.

macaque midbrain dopamine neurons (Stauffer et al., 2016) but of less duration than that of rat principal entorhinal neurons (Zhang et al., 2013). Thus it is likely that different cell types require different criterion for defining ChR2-responsive neurons. In our studies, we concluded that most of the neurons with latency greater than 10 ms had small to no change in firing rates during reward; none of the three neurons that increased firing rates to both reward and airpuff were under this category. We found that 7 of 27 VTA VGluT2 ChR2-responsive neurons had latencies greater than 10 ms, but the removal of these neurons from the dataset did not change our conclusion on segregating VTA VGluT2 neurons into neurons that are responsive to an aversive stimulus or neurons that are responsive to salience. This conclusion was also maintained in VTA VGluT2 ChR2-responsive neurons with latencies less than 6.5 ms. Thus, although it is possible that a minority of neurons categorized as ChR2 responsive were influenced by polysynaptic glutamate release, removal of these neurons does not change the conclusions of the study.

Two Major Subpopulations of VTA VGluT2 Neurons Based on Their Firing Patterns in Response to Rewarding or Aversive Stimuli

We identified a subpopulation of VTA VGluT2 neurons whose firing rates decreased in response to sucrose reward but increased in response to an aversive stimulus (airpuff). We suggest that the subpopulation of VTA VGluT2 neurons showing a decrease in firing rate in response to reward and an increase in response to airpuff signals aversion. These VTA VGluT2 neurons are likely to correspond to the previously identified "type III VTA neurons," which are shown to lack both dopaminergic and GABAergic phenotypes and are inhibited during reward but activated by airpuff (Cohen et al., 2012). One difference between our recordings of VTA VGluT2 neurons and type III VTA neurons is that type III VTA neurons begin decreasing firing rates during the delay period before reward, whereas we found that VTA VGluT2 neurons decrease firing rates at the time of reward port entry. Differences in the freely moving recording conditions performed here and the head-fixed recordings used to identify type III VTA neurons may be responsible for the observed difference in the onset of decreasing firing rates during reward-seeking behavior. Specifically, anticipatory licking behavior occurs in the delay period in the head-fixed recording preparation, whereas licking behavior occurs only following reward port entry in our freely moving preparation. Nevertheless, a role of VTA glutamatergic neurons in aversion is also congruent with electrophysiological recordings in anesthetized rats, showing that a population of non-dopaminergic neurons is excited by aversive stimuli (Ungless et al., 2004). Consistent with the participation of VTA VGluT2 neurons in aversion, optogenetic activation of fibers from VTA VGluT2 neurons within the lateral habenula or nucleus accumbens shell elicits aversive conditioning (Root et al., 2014a; Lammel et al., 2015; Qi et al., 2016). We also found that the baseline firing rates of VTA VGluT2 neurons were elevated in response to consecutive airpuff deliveries. This increased baseline firing of VTA VGluT2 neurons may reflect the anticipation of further aversive stimuli.

We identified, in addition to the VTA VGluT2 neurons that signal aversion, a subpopulation of VTA VGluT2 neurons whose firing rates are increased in response to both sucrose reward and airpuff. We suggest that this subpopulation of VTA VGluT2 neurons signals salient stimuli. It is unclear to what extent these glutamatergic neurons overlap with previously reported putative VTA dopamine neurons implicated in signaling salience in primates (Matsumoto and Hikosaka, 2009b; Bromberg-Martin et al., 2010). However, a recent study demonstrated that VTA glutamatergic neurons are intermingled with dopamine neurons in both nonhuman VTA and human VTA (Root et al., 2016), suggesting the possibility that some nonhuman primate midbrain salience signaling neurons are glutamatergic.

Two Major Subpopulations of VTA VGluT2 Neurons Based on Their Responses to Reward Expectation or the Presence of Reward

We found that most VTA VGluT2 neurons have greater changes in firing rate following reward port entries in response to the CS^+ compared with the CS^-, which suggests a differential expectation of reward. We further determined the extent to which changes in firing rate were due to the absence of reward during

CS^- trials or reward expectancy signaling by the CS^+ that mice learned to associate with sucrose delivery. By comparing the changes in firing rate following reward port entries in response to "CS^+ reward" trials (CS^+ paired to sucrose delivery during training days and recording sessions) and to "CS^E error" trials (CS^+ paired to sucrose delivery during training days but not during recording sessions) we identified two subpopulations of VTA VGluT2 neurons. In one of these subpopulations, we found that the firing rate of VTA VGluT2 neurons (approximately half of recorded neurons) did not differ between reward port entries for "CS^+ reward" trials and "CS^+ error" trials. Thus we conclude that this subpopulation of VTA VGluT2 neurons is responsive to the expectation of reward and suggest that these neurons correspond to the previously identified "type III" VTA neurons, shown to be non-dopaminergic, non-GABAergic, but responsive to the expectation of reward (Cohen et al., 2012). In the other subpopulation, we found that the changes in firing rate of VTA VGluT2 neurons (approximately half of recorded neurons) were greater during CS^+ reward trials compared with CS^+ error trials and suggest that this subpopulation of VTA VGluT2 neurons signals the presence of predicted reward.

Subpopulations of VTA VGluT2 Neurons Based on Their Response to Learned Cues or Reward Seeking

We found, in addition to the increase in firing rates by a major subpopulation of VTA VGluT2 neurons in response to airpuff, a small subpopulation of VTA VGluT2 neurons that selectively signals the CS^-. These patterns of responses by VTA VGluT2 neurons parallel those detected in neurons of non-human primate LHb, a structure innervated by VTA VGluT2 neurons (Root et al., 2014b, 2015a; Stamatakis et al., 2013) showing increased firing rates in response to CS^- in a reward task, or airpuff (Matsumoto and Hikosaka, 2009a). Thus the similarities in firing patterns by both VTA VGluT2 and LHb neurons in response to CS^- or aversive stimuli provide further evidence for the functional connectivity between VTA glutamatergic neurons and LHb neurons. Regarding functional connectivity between VTA VGluT2 neurons and LHb, several studies have shown that LHb photostimulation of fibers from VTA VGluT2 neurons is aversive (Lecca et al., 2017; Lammel et al., 2015; Root et al., 2014a), but see Yoo et al., 2016. A different subpopulation of VTA VGluT2 neurons was detected to signal both CS^+ and CS^-. The signaling to both CS^+ and CS^- has been previously observed in VTA neurons in primate and rabbit, although their phenotype was not defined (Matsumoto and Hikosaka, 2009b; Bromberg-Martin et al., 2010; Guarraci and Kapp, 1999).

We also detected a subpopulation of VTA VGluT2 neurons whose firing rates increased while mice were approaching the reward port. Similar approach-related changes in firing rate have been observed in ventral pallidal neurons (Root et al., 2013), which strongly regulate the VTA (Root et al., 2015b) and synapse onto VTA glutamate neurons (Faget et al., 2016). Thus we suggest that inputs from the ventral pallidum to VTA VGluT2 neurons are potentially part of a circuit underlying reward approach firing patterns.

Concluding Remarks

We electrophysiologically identified two major subpopulations of VTA VGluT2 neurons, a major subpopulation of VGluT2 neurons whose firing rate decreases in response to sucrose reward and increases in response to airpuff. This subpopulation may play a role in the aversive effects observed in response to optogenetic stimulation of axon terminals from VTA VGluT2 neurons (Root et al., 2014a; Lammel et al., 2015; Lecca et al., 2017; Qi et al., 2016). The other major subpopulation of VGluT2 neurons increases its firing rate in response to sucrose reward and in response to airpuff, suggesting that this subpopulation may play a role in the rewarding effects observed in response to VTA photostimulation of VGluT2 neurons (Wang et al., 2015; Yoo et al., 2016). We also identified a subpopulation of VTA VGluT2 neurons that changes its firing rate whether an expected reward is delivered or not, suggesting that this subpopulation signals reward expectation. We detected another subpopulation of VTA VGluT2 neurons that changes its firing rate when an expected reward is delivered but is unchanged when the expected reward is omitted, suggesting that this subpopulation of neurons signals the presence of reward. We found that some VTA VGluT2 neurons increase their firing rate in response to learned cues or actions to obtain sucrose reward. As VTA VGluT2 neurons are heterogeneous in their molecular composition and circuitry (Morales and Root, 2014; Root et al., 2014b; Qi et al., 2016; Wang et al., 2015), we suggest that this heterogeneity is likely to contribute to functional diversity among subpopulations of VTA VGluT2 neurons that signal different aspects of motivation.

METHODS

All methods can be found in the accompanying Transparent Methods supplemental file.

SUPPLEMENTAL INFORMATION

Supplemental Information includes Transparent Methods and can be found with this article online at https://doi.org/10.1016/j.isci.2018.03.008.

ACKNOWLEDGMENTS

This work was supported by the Intramural Research Program (IRP) of the National Institute on Drug Abuse (IRP/NIDA/NIH). Funding sources were not involved in study design, data collection, and interpretation, or in the decision to submit this research for publication. We thank NIDA Visual Media Services for figure preparation. Additionally, we thank Drs. Roy Wise, David Barker, Carlos Mejias-Aponte, and Flavia Barbano, as well as the entire Morales laboratory for their comments during the preparation of this manuscript.

AUTHOR CONTRIBUTIONS

D.H.R. and M.M. conceived this project. D.H.R. and D.J.E. performed experiments. D.H.R., D.J.E., and M.M. performed data analysis. D.H.R. and M.M. wrote the manuscript with the contribution of D.J.E.

DECLARATION OF INTERESTS

The authors declare no conflicts of interests.

Received: December 13, 2017
Revised: February 5, 2018
Accepted: February 22, 2018
Published: April 27, 2018

REFERENCES

Barker, D.J., Root, D.H., Zhang, S., and Morales, M. (2016). Multiplexed neurochemical signaling by neurons of the ventral tegmental area. J. Chem. Neuroanat. *73*, 33–42.

Bromberg-Martin, E.S., Matsumoto, M., and Hikosaka, O. (2010). Dopamine in motivational control: rewarding, aversive, and alerting. Neuron *68*, 815–834.

Cohen, J.Y., Haesler, S., Vong, L., Lowell, B.B., and Uchida, N. (2012). Neuron-type-specific signals for reward and punishment in the ventral tegmental area. Nature *482*, 85–88.

Dobi, A., Margolis, E.B., Wang, H.L., Harvey, B.K., and Morales, M. (2010). Glutamatergic and nonglutamatergic neurons of the ventral tegmental area establish local synaptic contacts with dopaminergic and nondopaminergic neurons. J. Neurosci. *30*, 218–229.

Faget, L., Osakada, F., Duan, J., Ressler, R., Johnson, A.B., Proudfoot, J.A., Yoo, J.H., Callaway, E.M., and Hnasko, T.S. (2016). Afferent inputs to neurotransmitter-defined cell types in the ventral tegmental area. Cell Rep. *15*, 2796–2808.

Guarraci, F.A., and Kapp, B.S. (1999). An electrophysiological characterization of ventral tegmental area dopaminergic neurons during differential pavlovian fear conditioning in the awake rabbit. Behav. Brain Res. *99*, 169–179.

Hnasko, T.S., Hjelmstad, G.O., Fields, H.L., and Edwards, R.H. (2012). Ventral tegmental area glutamate neurons: electrophysiological properties and projections. J. Neurosci. *32*, 15076–15085.

Kabanova, A., Pabst, M., Lorkowski, M., Braganza, O., Boehlen, A., Nikbakht, N., Pothmann, L., Vaswani, A.R., Musgrove, R., Di Monte, D.A., et al. (2015). Function and developmental origin of a mesocortical inhibitory circuit. Nat. Neurosci. *18*, 872–882.

Kawano, M., Kawasaki, A., Sakata-Haga, H., Fukui, Y., Kawano, H., Nogami, H., and Hisano, S. (2006). Particular subpopulations of midbrain and hypothalamic dopamine neurons express vesicular glutamate transporter 2 in the rat brain. J. Comp. Neurol. *498*, 581–592.

Kravitz, A.V., Owen, S.F., and Kreitzer, A.C. (2013). Optogenetic identification of striatal projection neuron subtypes during in vivo recordings. Brain Res. *1511*, 21–32.

Krishnan, V., Stoppel, D.C., Nong, Y., Johnson, M.A., Nadler, M.J., Ozkaynak, E., Teng, B.L., Nagakura, I., Mohammad, F., Silva, M.A., et al. (2017). Autism gene Ube3a and seizures impair sociability by repressing VTA Cbln1. Nature *543*, 507–512.

Lammel, S., Lim, B.K., and Malenka, R.C. (2014). Reward and aversion in a heterogeneous midbrain dopamine system. Neuropharmacology *76 Pt B*, 351–359.

Lammel, S., Lim, B.K., Ran, C., Huang, K.W., Betley, M.J., Tye, K.M., Deisseroth, K., and Malenka, R.C. (2012). Input-specific control of reward and aversion in the ventral tegmental area. Nature *491*, 212–217.

Lammel, S., Steinberg, E.E., Foldy, C., Wall, N.R., Beier, K., Luo, L., and Malenka, R.C. (2015). Diversity of transgenic mouse models for selective targeting of midbrain dopamine neurons. Neuron *85*, 429–438.

Lecca, S., Meye, F.J., Trusel, M., Tchenio, A., Harris, J., Schwarz, M.K., Burdakov, D., Georges, F., and Mameli, M. (2017). Aversive stimuli drive hypothalamus-to-habenula excitation to promote escape behavior. Elife *6*, e30697.

Matsumoto, M., and Hikosaka, O. (2009a). Representation of negative motivational value in the primate lateral habenula. Nat. Neurosci. *12*, 77–84.

Matsumoto, M., and Hikosaka, O. (2009b). Two types of dopamine neuron distinctly convey positive and negative motivational signals. Nature *459*, 837–841.

Morales, M., and Root, D.H. (2014). Glutamate neurons within the midbrain dopamine regions. Neuroscience *282*, 60–68.

Nieh, E.H., Matthews, G.A., Allsop, S.A., Presbrey, K.N., Leppla, C.A., Wichmann, R., Neve, R., Wildes, C.P., and Tye, K.M. (2015). Decoding neural circuits that control compulsive sucrose seeking. Cell *160*, 528–541.

Qi, J., Zhang, S., Wang, H.L., Barker, D.J., Miranda-Barrientos, J., and Morales, M. (2016). VTA glutamatergic inputs to nucleus accumbens drive aversion by acting on GABAergic interneurons. Nat. Neurosci. *19*, 725–733.

Root, D.H., Hoffman, A.F., Good, C.H., Zhang, S., Gigante, E., Lupica, C.R., and Morales, M. (2015a). Norepinephrine activates dopamine D4 receptors in the rat lateral habenula. J. Neurosci. *35*, 3460–3469.

Root, D.H., Ma, S., Barker, D.J., Megehee, L., Striano, B.M., Ralston, C.M., Fabbricatore, A.T., and West, M.O. (2013). Differential roles of ventral pallidum subregions during cocaine

self-administration behaviors. J. Comp. Neurol. *521*, 558–588.

Root, D.H., Mejias-Aponte, C.A., Qi, J., and Morales, M. (2014a). Role of glutamatergic projections from ventral tegmental area to lateral habenula in aversive conditioning. J. Neurosci. *34*, 13906–13910.

Root, D.H., Mejias-Aponte, C.A., Zhang, S., Wang, H.L., Hoffman, A.F., Lupica, C.R., and Morales, M. (2014b). Single rodent mesohabenular axons release glutamate and GABA. Nat. Neurosci. *17*, 1543–1551.

Root, D.H., Melendez, R.I., Zaborszky, L., and Napier, T.C. (2015b). The ventral pallidum: Subregion-specific functional anatomy and roles in motivated behaviors. Prog. Neurobiol. *130*, 29–70.

Root, D.H., Wang, H.L., Liu, B., Barker, D.J., Mod, L., Szocsics, P., Silva, A.C., Magloczky, Z., and Morales, M. (2016). Glutamate neurons are intermixed with midbrain dopamine neurons in nonhuman primates and humans. Sci. Rep. *6*, 30615.

Stamatakis, A.M., Jennings, J.H., Ung, R.L., Blair, G.A., Weinberg, R.J., Neve, R.L., Boyce, F., Mattis, J., Ramakrishnan, C., Deisseroth, K., and Stuber, G.D. (2013). A unique population of ventral tegmental area neurons inhibits the lateral habenula to promote reward. Neuron *80*, 1039–1053.

Stauffer, W.R., Lak, A., Yang, A., Borel, M., Paulsen, O., Boyden, E.S., and Schultz, W. (2016). Dopamine neuron-specific optogenetic stimulation in rhesus macaques. Cell *166*, 1564–1571.e6.

Tan, K.R., Yvon, C., Turiault, M., Mirzabekov, J.J., Doehner, J., Labouebe, G., Deisseroth, K., Tye, K.M., and Luscher, C. (2012). GABA neurons of the VTA drive conditioned place aversion. Neuron *73*, 1173–1183.

Taylor, S.R., Badurek, S., Dileone, R.J., Nashmi, R., Minichiello, L., and Picciotto, M.R. (2014). GABAergic and glutamatergic efferents of the mouse ventral tegmental area. J. Comp. Neurol. *522*, 3308–3334.

Ungless, M.A., Magill, P.J., and Bolam, J.P. (2004). Uniform inhibition of dopamine neurons in the ventral tegmental area by aversive stimuli. Science *303*, 2040–2042.

van Zessen, R., Phillips, J.L., Budygin, E.A., and Stuber, G.D. (2012). Activation of VTA GABA neurons disrupts reward consumption. Neuron *73*, 1184–1194.

Viereckel, T., Dumas, S., Smith-Anttila, C.J., Vlcek, B., Bimpisidis, Z., Lagerstrom, M.C., Konradsson-Geuken, A., and Wallen-Mackenzie, A. (2016). Midbrain gene screening identifies a new mesoaccumbal glutamatergic pathway and a marker for dopamine cells neuroprotected in Parkinson's disease. Sci. Rep. *6*, 35203.

Wang, H.L., Qi, J., Zhang, S., Wang, H., and Morales, M. (2015). Rewarding effects of optical stimulation of ventral tegmental area glutamatergic neurons. J. Neurosci. *35*, 15948–15954.

Wise, R.A. (2004). Dopamine, learning and motivation. Nat. Rev. Neurosci. *5*, 483–494.

Yamaguchi, T., Qi, J., Wang, H.L., Zhang, S., and Morales, M. (2015). Glutamatergic and dopaminergic neurons in the mouse ventral tegmental area. Eur. J. Neurosci. *41*, 760–772.

Yamaguchi, T., Sheen, W., and Morales, M. (2007). Glutamatergic neurons are present in the rat ventral tegmental area. Eur. J. Neurosci. *25*, 106–118.

Yamaguchi, T., Wang, H.L., Li, X., Ng, T.H., and Morales, M. (2011). Mesocorticolimbic glutamatergic pathway. J. Neurosci. *31*, 8476–8490.

Yoo, J.H., Zell, V., Gutierrez-reed, N., Wu, J., Ressler, R., Shenasa, M.A., Johnson, A.B., Fife, K.H., Faget, L., and Hnasko, T.S. (2016). Ventral tegmental area glutamate neurons co-release GABA and promote positive reinforcement. Nat. Commun. *7*, 13697.

Zhang, S., Qi, J., Li, X., Wang, H.L., Britt, J.P., Hoffman, A.F., Bonci, A., Lupica, C.R., and Morales, M. (2015). Dopaminergic and glutamatergic microdomains in a subset of rodent mesoaccumbens axons. Nat. Neurosci. *18*, 386–392.

Zhang, S.J., Ye, J., Miao, C., Tsao, A., Cerniauskas, I., Ledergerber, D., Moser, M.B., and Moser, E.I. (2013). Optogenetic dissection of entorhinal-hippocampal functional connectivity. Science *340*, 1232627.

ISCI, Volume *2*

Supplemental Information

Aversion or Salience Signaling by Ventral Tegmental Area Glutamate Neurons

David H. Root, David J. Estrin, and Marisela Morales

Supplemental Information

Transparent methods

All animal procedures were performed in accordance with the National Institutes of Health Guidelines, and approved by the National Institute on Drug Abuse Animal Care and Use Committee.

Subjects. Male VGluT2-IRES::Cre mice were used (n = 14, 25-30g body weight; *Slc17a6*$^{tm2(cre)Lowl/J}$ in C57BL/6J background from The Jackson Laboratories, Bar Harbor, ME).

Surgical procedures. Mice were anesthetized with 1–5% isofluorane. AAV5-EF1α-DIO-hChR2(H134R)-eYFP (UNC Vector Core, Chapel Hill, North Carolina USA) was injected (350 nl) in the VTA [-3.3 mm anteroposterior (AP), 0.0 mm mediolateral (ML), -4.3 mm dorsoventral (DV)] at a flow rate of 100 nl/min. Injections were made using the UltraMicroPump, Nanofil syringes, and 35 g needles (World Precision Instruments, Sarasota, FL USA). Syringes were left in place for 10 min following injections to minimize diffusion. At least 3 weeks after virus injection, mice were implanted with microwire electrodes in the midbrain (-2.9 to -3.8 AP, -0.2 to 1.5 ML at 10º angle, -4.5 DV; Microprobes, Gaithersberg MD USA) (Barker et al., 2014). The microwire array consisted of a 4 x 4 array of polymide-coated stainless steel microelectrodes (25 µm diameter) surrounding a 200 µm multimode optical fiber (**Figure 1**). Electrodes were separated by 250 µm anterior to posterior and medial to lateral, except for the electrodes closest to the optical fiber, which were separated by 500-600 µm. The optical fiber was approximately 500 µm dorsal to the electrode tips. An additional stainless-steel electrode was implanted 250 µm posterior to the optical fiber and used in conjunction with a stainless-steel electrode wrapped around a stainless-steel screw implanted in the skull as a ground.

Apparatus. Mice were trained in a 7”W x 7”D x 12”H conditioning chamber (Mouse Test Cage, Coulbourn, Holliston, MA USA) within a sound attenuating cubicle (ENV-018V, Med-Associates, Fairfax, VT USA). A syringe pump (PHM-100, Med-Associates) delivered 8% sucrose to a custom-made plastic reward port with infrared head entry detector (ENV-302HD, Med-Associates). Auditory cues were delivered by a programmable audio generator (ANL-926, Med-Associates).

Behavioral procedures. One week following electrode implantation, mice were restricted to 85% free-feeding body weight for the duration of all behavioral experiments. Two days prior to training, mice were pre-exposed to 8% sucrose in their home cage for 1 hour. One day prior to training, mice were placed in the conditioning chamber and delivered 8% sucrose (40 µl) every 30 sec for 30 min. On day 1 of training, mice were placed in the conditioning chamber for 2 h, and a conditioned stimulus, CS^+ (7000 Hz, 80 dB, 10 sec duration) predicting 8% sucrose was delivered at 0 and 5 sec after CS^+ onset (20 µl at each delivery). A different conditioned stimulus, CS^- (white noise, 80 dB, 10 sec duration), did not result in sucrose delivery. Cues were presented with a variable 25-45 sec inter-trial interval. The same training procedure was used for electrophysiological recordings, except that the CS^+ tone resulted in sucrose delivery on 90% of CS^+ trials. On 10% of randomly distributed CS^+ presentations, the CS^+ tone was played without sucrose delivery. These trials were termed CS^+ error trials (CS^E). Following the reward task recordings, access to the port was blocked, and the same mice were exposed to 20-30 airpuffs of nitrogen delivered to the face with a distance of approximately 4 cm from the snout (25 PSI, 200 ms duration, Picospritzer III, Parker, Pine Brook NJ USA). Following airpuff delivery, fiber optic ferrules were connected to a rotary joint (Doric Lenses, Quebec, Quebec Canada) and 473 nm light pulses (1 Hz, 5 ms, 10-20 mW) were delivered.

Electrophysiological and video recordings. Neural discharges were amplified and digitized within a headstage (ZD32, TDT, Alachua FL USA), routed through a motorized commutator (ACO32, TDT), differentially amplified against another microwire that did not exhibit a single unit (PZ4, TDT), bandpass filtered 300-5000 Hz, and acquired in software at 25 kHz/channel (OpenWorkbench and OpenController, TDT). Video recordings synchronized with neuronal acquisition clocks were acquired at 30 Hz (RV2, TDT).

Behavioral video analysis. Frame by frame timestamps were overlayed onto video files by Avidemux v2.6 and recorded for approaches toward the reward port in MPC-HC v1.7.10. Approach onset was determined by the start of a change in direction toward the reward port and approach offset was the breaking of the reward port photocell (Root et al., 2013). Approach onset was typically a leftward or rightward head turn, or the start of

alternating limb movements toward the reward port. Approaches greater than 3 seconds in duration were excluded from analysis.

Optogenetic classification. We used organized arrays of microwires with optical fibers similar to those used by Kravitz and colleagues (Kravitz et al., 2013). Optical Microwire Arrays allow for verification of individual recording sites within brain tissue (Barker et al., 2014). However, this organization causes light to be delivered more strongly to microwires proximal to the fiber and less to microwires distal to the fiber (Kravitz et al., 2013). To account for differences in light distribution, individual wires were recorded at increasing light intensities (mW). For each neuron, the light intensity that generated the shortest latency responses and highest fidelity was designated as the optimal light intensity (Kravitz et al., 2013). After identification of optimal light intensity, we classified single-units as channelrhodopsin (ChR2)-responsive by the following criterion: (1) median latency to fire less than 15 ms following light onset (Kravitz et al., 2013) and (2) greater than 60% fidelity to fire an action potential following light onset.

Electrophysiological analyses. Isolation and separation of individual neural waveforms from background noise and waveforms of other neurons recorded from the same microwire were conducted offline using spike sorting and separation software (SciWorks, DataWave, Loveland CO USA) as previously described (Root et al., 2013). Neural discharges were sorted by waveform parameters, including principal components 1 through 3, peak voltage, spike height, peak voltage time, and voltages at user-defined time cursors. Interspike interval histograms were constructed for each neuron to confirm that no discharges occurred during refractory period (<1.8ms). Cross-correlations were used to confirm that populations of neurons from single microwires were distinct neurons. Waveforms exhibiting signal-to-noise ratios less than 2:1 were discarded. Each mouse was recorded one or two times, typically separated by 5 or 6 days if recorded twice. When similar mean waveform and interspike interval histograms patterns were recorded from the same microwire on both days (Coffey et al., 2015), only one recording was included in the dataset of optogenetically-identified neurons.

Changes in firing rate were computed using a standardized change ratio, (E – B) / (E + B), where B is the mean baseline firing rate across trials and E is the mean event firing rate across trials. Using this standardized change ratio a 50% change from baseline firing rate during an event equals 0.20 (increase) or -0.20 (decrease), and no change in firing from baseline equals 0. To examine changes in firing rate in response to the CS^+ or CS^-, B equaled the firing rate -150 to 0 ms prior to all cue presentations (cue baseline), and E equaled the firing rate between 0-150 ms following CS^+ or CS^-. The 150 ms duration for cue baseline was chosen to assess firing based on cue presentation without influence of cue-induced movements (Ghitza et al., 2003). To examine changes in firing rate prior to and following reward-seeking behaviors, B equaled the firing rate from -6 to -3 sec prior to reward port entries (movement baseline), determined by infrared photobeam breaks, and E equaled the firing rate -2 to 0 sec prior to reward port entry (pre-reward) or 0 to 2 sec following reward port entry (post-reward). If reward port entries occurred within 3 sec of each other they were discarded from neural examination. Reward port entries were divided into all reward port entries, trials in which the CS^+ was played and sucrose was delivered, trials in which the CS^- was played without sucrose delivery, or CS^E trials in which the CS^+ played but sucrose was not delivered. Two VTA VGluT2 neurons were recorded without CS^E trials. In select analyses, we directly compared the changes in firing rate between two behaviorally matched events under different reward expectation circumstances. To compare the changes in firing rate following reward port entry during CS^+ and CS^E trials, (E – B) / (E + B), B = the firing rate 0-2 sec following reward port entry on CS^+ trials, and E = the firing rate 0 to 2 sec following reward port entry on CS^E trials. To examine changes in firing rate in response to the airpuff, A equaled the firing rate 200 to 0 ms prior to airpuffs, and B equaled the firing rate 0 to 200 ms during airpuffs.

***Histology*.** Mice were anesthetized with 1-5% isoflurane and anodal current (50 µA, 2 sec) was passed through each microwire to mark the tip location. Mice were then perfused with phosphate buffer (PB, 0.1M, pH 7.4) followed by 4% paraformaldehyde. The brain was extracted and stored in 4% paraformaldehyde for 2h prior to storing overnight in 18% sucrose at 4ºC. Brains were coronally sectioned (40 µm) through the VTA and processed for tyrosine hydroxylase (TH) immunohistochemistry to identify the borders of the VTA. VTA sections were washed in PB, treated with 0.01% H_2O_2 for 15 min before washing again in PB, pretreated for 1 h in blocking buffer (PB supplemented with 0.1% Triton X-100 and 4% bovine serum albumin), and incubated overnight at 4ºC with blocking buffer supplemented with mouse anti-TH (1:1000, MAB318, Millipore, Burlington, MA USA, RRID:AB_2201528). Brains were then washed in PB, incubated for 1h at room

temperature with blocking buffer supplemented with goat anti-mouse biotinylated secondary (BA1000, 1:200, Vector Labs, Burlingame, CA USA), washed in PB, incubated for 1h at room temperature with PB supplemented with avidin-biotinylated horseradish peroxidase (1:200, ABC kit, Vector Labs). Sections were washed in PB and peroxidase reaction was developed with 0.05% 3,3'-diaminobenzidine tetrahydrochloride and 0.003% H_2O_2. To identify recording sites, sections were mounted on coated slides and incubated in 5% potassium ferrocyanide and 10% HCl. Sections were imaged by a VS120 (Olympus, Center Valley, PA USA) microscope at 20X. The positions of the microwires were identified by their tracks in the brain and the blue potassium ferrocyanide iron deposits. Recordings from microwires localized outside of the tyrosine hydroxylase-labeled VTA were not included. Subdivisions of the VTA were identified based on prior research of tyrosine hydroxylase immunoreactions (Root et al., 2014) and mouse brain atlas (Paxinos and Franklin, 2001).

***Statistics*.** A 2 (CS) x 2 (Day) repeated measures ANOVA was used to examine acquisition of the reward task. Sidak-adjusted pairwise comparisons evaluated specific changes between days and cues. Paired t-tests were used to evaluate changes in standardized changes in firing rate between two variables. Correlation coefficients of changes in firing rate between two variables were compared by Fisher's r-to-z transformation followed by asymptotic covariance tests (Steiger, 1980, Lee and Preacher, 2013). A hierarchical clustering analysis and K-means principle component analysis was used to determine if neurons clustered into subpopulations based on their changes in firing rate following reward port entries during CS^+ trials and their changes in firing rate in response to the airpuff. Inspection of the scree plot "elbow" was used to determine number of clusters. Heat plots were constructed in Matlab (Mathworks) using the standardized change in firing rate formula (E – B) / (E + B), where B was baseline and E was each bin of the perievent time histogram for an event. Movement or airpuff bins were 50 ms and cue bins were 10 ms. All tests were performed in SPSS (SPSS, IBM, Armonk NY USA) except cluster analyses, which were performed in R.

References

BARKER, D. J., ROOT, D. H., COFFEY, K. R., MA, S. & WEST, M. O. 2014. A procedure for implanting organized arrays of microwires for single-unit recordings in awake, behaving animals. *J Vis Exp*, e51004.

COFFEY, K. R., BARKER, D. J., GAYLIARD, N., KULIK, J. M., PAWLAK, A. P., STAMOS, J. P. & WEST, M. O. 2015. Electrophysiological evidence of alterations to the nucleus accumbens and dorsolateral striatum during chronic cocaine self-administration. *Eur J Neurosci,* 41**,** 1538-52.

GHITZA, U. E., FABBRICATORE, A. T., PROKOPENKO, V., PAWLAK, A. P. & WEST, M. O. 2003. Persistent cue-evoked activity of accumbens neurons after prolonged abstinence from self-administered cocaine. *J Neurosci,* 23**,** 7239-45.

KRAVITZ, A. V., OWEN, S. F. & KREITZER, A. C. 2013. Optogenetic identification of striatal projection neuron subtypes during in vivo recordings. *Brain Res,* 1511**,** 21-32.

LEE, I. & PREACHER, K. 2013. *Calculation for the test of the difference between two dependent correlations with one variable in common [Computer software], September 2013.*

PAXINOS, G. & FRANKLIN, K. B. J. 2001. *The mouse brain in stereotaxic coordinates,* San Diego, Academic Press.

ROOT, D. H., MA, S., BARKER, D. J., MEGEHEE, L., STRIANO, B. M., RALSTON, C. M., FABBRICATORE, A. T. & WEST, M. O. 2013. Differential roles of ventral pallidum subregions during cocaine self-administration behaviors. *J Comp Neurol,* 521**,** 558-88.

ROOT, D. H., MEJIAS-APONTE, C. A., ZHANG, S., WANG, H. L., HOFFMAN, A. F., LUPICA, C. R. & MORALES, M. 2014. Single rodent mesohabenular axons release glutamate and GABA. *Nat Neurosci,* 17**,** 1543-51.

STEIGER, J. H. 1980. Tests for comparing elements of a correlation matrix. *Psychological bulletin,* 87**,** 245.